Pharmaceutical Sciences and Drug Design
ISSN: 3062-4428
2025, Volume 5, Page No: 1-19

Available online at: www.galaxypub.co/page/journals

Galaxy Publication

ED-71 Protects Against Glucocorticoid-Triggered Osteoporosis by Influencing Osteoblast Differentiation through Notch and Wnt/β-Catenin Pathways

Haruto Watanabe[1]*, Akira Mori[1]

[1]Department of Pharmacognosy, Faculty of Pharmaceutical Sciences, Tohoku University, Sendai, Japan.

***E-mail** ✉ haruto.w.jp@gmail.com

Received: 05 October 2024; **Revised:** 08 January 2025; **Accepted:** 11 January 2025

ABSTRACT

Prolonged exposure to glucocorticoids frequently results in glucocorticoid-induced osteoporosis (GIOP). This work investigated whether eldecalcitol (ED-71), a new active analog of vitamin D3, can counteract GIOP and sought to clarify the molecular pathways responsible for its protective action. A GIOP mouse model was generated by administering methylprednisolone (MPED) or dexamethasone (DEX) intraperitoneally to C57BL/6 mice, while ED-71 was concurrently delivered by oral gavage. Bone morphology, microarchitectural characteristics, newly synthesized bone, and osteogenic marker expression were assessed using HE staining, micro-CT, calcein/tetracycline double labeling, and IHC analysis. In vitro experiments employed MC3T3-E1 pre-osteoblasts exposed to DEX, and osteogenic differentiation and mineral deposition were examined through ALP staining, AR staining, qPCR, Western blotting, and immunofluorescence. ED-71 alleviated the loss of bone mass and defects in microstructural parameters observed in GIOP mice, while simultaneously enhancing bone formation and stimulating osteoblast function, accompanied by suppression of osteoclast activity. In cultured MC3T3-E1 cells, ED-71 restored osteogenic differentiation and mineralization hindered by DEX and markedly increased the expression of osteogenesis-associated molecules. ED-71 exposure also elevated GSK3-β and β-catenin levels while diminishing Notch expression. The use of the Wnt pathway inhibitor XAV939 or forced Notch activation eliminated the pro-osteogenic influence of ED-71. ED-71 counteracts GIOP by promoting osteogenic differentiation through coordinated modulation of Notch and Wnt/GSK-3β/β-catenin signaling pathways. These findings indicate that ED-71 holds promising translational potential as a therapeutic strategy for preventing GIOP.

Keywords: Wnt/GSK-3β/β-catenin signaling, Gucocorticoid-induced osteoporosis, Eldecalcitol, Notch signaling, osteoblasts

How to Cite This Article: Watanabe H, Mori A. ED-71 Protects Against Glucocorticoid-Triggered Osteoporosis by Influencing Osteoblast Differentiation through Notch and Wnt/β-Catenin Pathways. Pharm Sci Drug Des. 2025;5:1-19. https://doi.org/10.51847/aqKnaGGMQB

Introduction

Glucocorticoids remain indispensable as anti-inflammatory and immunosuppressive agents for treating chronic inflammatory disorders, allergic conditions, and for preventing organ transplant rejection [1]. However, their broad clinical application has made glucocorticoid-induced osteoporosis (GIOP) an increasingly significant complication. Evidence indicates that nearly one-third of individuals receiving glucocorticoid therapy for six months or more may develop osteoporosis [2]. GIOP represents the third major contributor to pathological skeletal deterioration after age-related and postmenopausal bone loss, accounting for osteoporosis in close to 20% of affected patients [3]. The condition is characterized by abrupt reductions in bone mass and a dose-dependent elevation in fracture susceptibility occurring early in the treatment course [1, 4]. Although it is the most prevalent form of drug-related osteoporosis, it has received far less mechanistic investigation than postmenopausal osteoporosis, and the absence of mechanistically targeted therapeutics continues to be a barrier to optimal management [5].

Unlike postmenopausal osteoporosis—which is driven largely by heightened osteoclast activity—GIOP develops through a fundamentally different mechanism. Glucocorticoids suppress bone formation by impairing osteoblast proliferation, differentiation, and functional maturation, in addition to triggering apoptosis in both osteoblasts and

osteocytes [6, 7]. They also enhance osteoclastogenesis and early bone resorption, before ultimately suppressing both osteoblasts and osteoclasts during prolonged exposure [8]. Current GIOP management relies heavily on pharmacologic options such as bisphosphonates, teriparatide, and denosumab, yet their effectiveness remains suboptimal [2]. Consequently, coupling glucocorticoid treatment with adjunctive pharmacologic intervention is considered essential for reducing the likelihood or severity of GIOP.

Active vitamin D, synthesized through hepatic and renal metabolism, has long been used alongside calcium as an initial preventive measure for GIOP [9]. Beyond its classical roles in maintaining calcium–phosphorus balance and promoting mineralization, activated vitamin D directly influences osteoblasts and indirectly regulates osteoclasts by modulating osteoblast-derived signals [10]. Eldecalcitol (ED-71), a recently developed active vitamin D3 analog approved in Japan, has shown superior pharmacokinetic stability compared with conventional vitamin D forms, owing to its longer half-life and stronger interaction with vitamin D–binding proteins [11, 12]. It has been documented to lower fracture risk [13], diminish bone turnover, mitigate bone loss in ovariectomized (OVX) models [14], and reduce trabecular deterioration and fragility in rodent models of type I diabetes [15]. Our earlier work also demonstrated multiple protective roles of ED-71, including stimulation of mini-modeling in OVX rats [16], improvement of diabetic osteoporosis via immune modulation [17], attenuation of cyclophosphamide-induced osteoporosis [18], and enhancement of bone regeneration in defect models [19]. Clinical studies have further noted that ED-71 surpasses alfacalcidol in maintaining bone mineral density among GIOP patients [20], yet the mechanisms responsible for its beneficial effects remain poorly defined, and it is not fully established whether ED-71 can prevent the onset and progression of GIOP.

The Notch signaling cascade, triggered through ligand–receptor interactions and known to regulate downstream genes such as Hes1 and Hey1, functions as a key regulator of cell–cell communication [21]. Aberrant activation of Notch contributes to osteoporosis by suppressing osteoblast differentiation during bone remodeling [22], and experimental inhibition of this pathway enhances osteogenesis in OVX models [23]. Glucocorticoids have been reported to increase Notch1 transcription in osteoblasts, thereby diminishing osteoblast functionality in GIOP [24]. In parallel, the canonical Wnt/β-catenin pathway plays a crucial role in skeletal homeostasis [25]. Wnt ligands engage Frizzled (FZD) receptors and the co-receptors LRP-5/6 to stabilize β-catenin, enabling its nuclear translocation and activation of Wnt-responsive genes [26], ultimately directing mesenchymal stem cells toward osteogenic commitment [27]. Activation of Wnt/GSK-3β/β-catenin signaling has also been shown to counteract the suppressive effects of dexamethasone on MC3T3-E1 cells, promoting proliferation, differentiation, and mineralization [28], implicating this pathway as a potential therapeutic target for GIOP. Interaction between Notch and Wnt pathways is well recognized in contexts such as muscle development, liver disease, and cancer biology [29, 30]. GSK-3β, for example, has been identified as a molecular node linking these pathways during myogenesis [30]. Moreover, physiologic bone cell maturation depends on a balance characterized by elevated Notch activity and relatively subdued Wnt signaling [31]. Whether these intertwined pathways contribute to the protective effects of ED-71 in GIOP, however, has yet to be determined.

To address these gaps, the present study established a GIOP mouse model to assess the preventive actions of ED-71 in vivo. Complementary in vitro experiments were employed to investigate whether ED-71 mitigates GIOP by modulating Notch and Wnt/β-catenin signaling to enhance osteoblast differentiation. Collectively, this work aims to uncover mechanistic targets relevant to osteoporosis—including GIOP—and to inform new therapeutic avenues for its clinical management.

Materials and Methods

Establishment of the GIOP mouse model and ED-71 administration

Male C57BL/6 mice (eight weeks old) were obtained from Jinan Pengyue Laboratory Animal Breeding Co., Ltd. (Jinan, China) and housed under standard environmental conditions with a 12-hour light–dark cycle. All procedures followed the National Institutes of Health Guidelines for the Care and Use of Laboratory Animals and were authorized by the Institutional Animal Care and Use Committee of the School and Hospital of Stomatology, Shandong University (IACUC No. 20210915).

The animals were randomly divided into six experimental groups (n=8):

1. CON (4-week protocol),
2. MPED,
3. MPED+ED-71,

4. CON (8-week protocol),
5. DEX,
6. DEX+ED-71.

To generate the GIOP model, the MPED and MPED+ED-71 groups received daily intraperitoneal injections of methylprednisolone (10 mg/kg; MedChemExpress, USA) for four weeks. Mice in the MPED+ED-71 cohort were simultaneously treated with oral ED-71 at 50 mg/kg/day, following a previously described regimen [19].
For the eight-week model, the DEX and DEX+ED-71 groups were administered daily intraperitoneal dexamethasone (1 mg/kg; MedChemExpress). Animals in the DEX+ED-71 group were given 50 mg/kg/day ED-71 by oral gavage throughout the duration of treatment.
At the study endpoint, a subset of mice was anesthetized and euthanized via cervical dislocation. Their femurs were harvested and fixed in 75% ethanol for micro-computed tomography (micro-CT) or used to prepare undecalcified sections. The remaining mice underwent intracardiac perfusion with 4% paraformaldehyde. After fixation, femurs were decalcified at 4°C in EDTA-2Na for four weeks, dehydrated through graded ethanol, embedded in paraffin, and sectioned at 5 μm thickness for subsequent histological analyses.

Micro-CT evaluation
After 4 or 8 weeks of intervention, femoral trabecular architecture was evaluated using a SCANCO Medical micro-CT system (SCANCO Medical AG, Switzerland). Images were obtained at a 10 μm voxel size, and two- and three-dimensional reconstructions were generated using the manufacturer's analysis software.

Calcein and tetracycline double labeling
To assess dynamic bone formation, mice received tetracycline (20 mg/kg) and calcein (8 mg/kg) subcutaneous injections 13 and 3 days before sacrifice, respectively [16]. Following anesthesia and euthanasia, femurs were fixed in 75% ethanol for 48 hours, embedded in hard-tissue media, and sectioned into 100–200 μm slices under low-light conditions. Fluorescent signals corresponding to mineral apposition were visualized beneath the distal femoral growth plate using a BX-53 fluorescence microscope (Olympus, Japan).

Hematoxylin and eosin (HE) staining
For histological evaluation, paraffin sections were deparaffinized, hydrated, stained with hematoxylin for 15 minutes, rinsed, incubated in eosin for 7 minutes, dehydrated, and mounted. Images were captured under an Olympus BX-53 microscope. Using Image-Pro Plus 6.2 (Media Cybernetics, USA), trabecular bone parameters—BV/TV, Tb.Th, Tb.N, and Tb.Sp—were quantified. For each bone sample, three independent levels (two margins and one central region) were analyzed, and parallel sections were averaged. Comparisons were made against level-matched CON tissues.

Immunohistochemistry (IHC) and TRAP staining
To assess osteogenic and osteoclastic activity, immunohistochemical staining was conducted for ALP, OCN, RUNX2, and COL1. After deparaffinization, endogenous peroxidase was blocked with 0.3% hydrogen peroxide for 30 minutes. Sections were then incubated in 1% BSA/PBS for 20 minutes to reduce nonspecific binding. Primary antibodies—anti-ALP (1:150, ab108337), anti-OCN (1:150, ab93876), anti-RUNX2 (1:50, ab192256), and anti-COL1 (1:100, ab34710) (all from Abcam, UK)—were applied overnight at 4°C. The following day, sections were incubated with HRP-conjugated secondary antibody (1:200, ab6721, Abcam) for 1 hour at room temperature. Diaminobenzidine (Sigma-Aldrich, Germany) was used for visualization.
To examine osteoclast activity, ALP&TRAP double staining was performed. After ALP staining, sections were rinsed and processed with TRAP solution for 15 minutes at room temperature until characteristic red coloration was visible. Methyl green counterstaining was applied before microscopy.
For semiquantitative analysis, three sections per sample (margin, center, margin) were evaluated using Image-Pro Plus 6.2. RUNX2-positive osteoblasts and TRAP-positive osteoclasts were counted, while the mean optical density of ALP and OCN and the integrated optical density of COL1 were measured across three randomly selected non-overlapping fields.

Cell culture, osteogenic differentiation, and drug exposure
MC3T3-E1 pre-osteoblasts (Shanghai Cell Center, China) were cultured in α-MEM supplemented with 10% fetal bovine serum, 100 U/mL penicillin, and 100 μg/mL streptomycin at 37°C in a humidified 5% CO_2 atmosphere.

To induce osteogenic differentiation, cells were transferred to differentiation medium containing 50 mg/L ascorbic acid, 100 mM β-glycerophosphate, and 10 nM DEX [23], and maintained for 7, 14, or 21 days with media replaced every three days. For GIOP-mimicking conditions, cells were exposed to DEX (1 μM) [32] alone or co-treated with DEX and ED-71 (1 nM) [17] during the differentiation period.

XAV939 treatment and hes1 overexpression

To suppress Wnt/β-catenin signaling, MC3T3-E1 cells were exposed to the β-catenin inhibitor XAV939 (10 μM, MedChemExpress).32 Cells receiving only dimethyl sulfoxide served as the control group. Activation of the Notch pathway was achieved by introducing a Hes1 overexpression construct (pcDNA3.4–3xflag carrying NM_008235), synthesized by Keyybio (Shandong, China). Following the manufacturer's directions, the plasmid (4 μg per 2 mL medium) was delivered into MC3T3-E1 cells with the ZLip2000 transfection reagent (10 μL per 2 mL; Zoman Biotechnology, Beijing, China). A separate batch of cells transfected with the empty pcDNA3.4–3xflag vector (4 μg/2 mL) acted as the baseline control. All experimental and control cells were maintained in six-well culture plates.

Immunofluorescence staining

For immunostaining, MC3T3-E1 cells were first immobilized in 4% paraformaldehyde for 20 min, followed by blocking in PBS containing 5% BSA for 1 h. Cells were then incubated overnight with primary antibodies targeting β-catenin (1:200; ab32572, Abcam) or Notch1 (1:200; ab52627, Abcam). The subsequent day, an Alexa Fluor® 488–conjugated secondary antibody (1:200; ab150081, Abcam) was applied for 1 h. Nuclear staining was performed using 4′,6-diamidino-2-phenylindole. Fluorescent images were finally obtained using an Olympus BX-53 fluorescence microscope.

ALP staining and alizarin red (AR) staining

To assess early osteogenic activity, MC3T3-E1 cells were cultured in an osteogenic induction medium for seven days, then fixed in 4% paraformaldehyde for 20 min. ALP activity was visualized using the ALP staining solution (Solarbio, Beijing, China) according to the manufacturer's protocol. For each experimental condition, at least three culture plates were evaluated, with five randomly chosen fields per plate. Images were captured using an Olympus CKX-41 optical microscope.

For AR staining, cells were maintained in osteogenic induction medium for 21 days to allow mineralized nodule formation. After fixation in 4% paraformaldehyde, the cultures were stained with 1% AR solution (Lot No. 20180820, Solarbio) to quantify mineral deposition. As with ALP staining, a minimum of three plates per group and five randomly selected fields per plate were examined. Imaging was carried out with the Olympus CKX-41 microscope.

Real-time polymerase chain reaction (RT-qPCR) analysis

After seven days of culture, the medium was removed from MC3T3-E1 cells and the monolayers were washed three times with chilled PBS in preparation for total RNA isolation. RNA was extracted using Trizol reagent (AG21102, Accurate Biotechnology, China). cDNA synthesis was performed with the Evo M-MLV RT Reverse Transcription Kit II (AG11711, Accurate Biotechnology), following the manufacturer's protocol. RT-qPCR reactions were carried out using the SYBR Green Pro Taq HS premixed kit (AG11701, Accurate Biotechnology) on a LightCycler® 96 system (Roche, Switzerland). GAPDH served as the internal reference gene, and relative expression levels were determined using the $2^{-\Delta\Delta Cq}$ method with GraphPad Prism 6.0 (GraphPad Inc., San Diego, CA, USA). Primer sequences are listed in **Table 1**.

Table 1. Specific Primers for Control and Target Genes

Gene	Forward	Reverse
COL1	5'-TGGAAGAGTGGAGAGTACTGGAT −3'	5'-ATACTCGAACTGGAATCCATCGG −3'
ALP	5'- TCAGGGCAATGAGGTCACATC −3'	5'- CACAATGCCCACGGACTTC −3'
RUNX2	5'- CGGCCCTCCCTGAACTCT −3'	5'- TGCCTGCCTGGGATCTGTA −3'
OSX	5'-CTTGGGAACACTGAAGCTGT −3'	5'- CTGTCTTCACCTCAATTCTATT −3'
OCN	5'-TCTGACCTCACAGATGCCAAG −3'	5'- AGGGTTAAGCTCACACTGCT-3'

β-catenin	5'-CCTAGCTGGTGGACTGCAGAA-3	5'-CACCACTGGCCAGAATGATGA-3
Notch1	5'-CCAAGCAAGAAGCGGAGAG −3'	5'- TGTCGTCCATCAGAGCACCAT-3'
GAPDH	5'-GGTGAAGGTCGGTGTGAACG-3	5'-CTCGCTCCTGGAAGATGGTG-3

Western blotting

Protein extraction was carried out using RIPA lysis buffer (Lot 02408/60412, CwBio Biotechnology Co., Ltd., China) following the supplier's protocol. The total protein concentration was determined with a bicinchoninic acid assay kit (P0012S, BeyoTime Biotechnology, Shanghai, China). After quantification, samples were combined with one-quarter volume of 5× sodium dodecyl sulfate loading buffer and denatured at 95 °C for 5 min. The denatured samples were resolved on 10% sodium dodecyl sulfate–polyacrylamide gels, followed by transfer onto polyvinylidene fluoride membranes. Membranes were blocked with 5% BSA prepared in TBST for 1 h at room temperature and then exposed to primary antibodies, including anti-GAPDH (ab9485, Abcam), anti-COL1 (ab34710, Abcam), anti-ALP (ab108337, Abcam), anti-RUNX2 (ab192256, Abcam), anti-OCN (ab93876, Abcam), anti-Notch1 (ab52627, Abcam), anti-p-GSK-3β (ab131097, Abcam), anti-β-catenin (ab32572, Abcam), anti-non-phospho (Active) β-Catenin (8814, Cell Signaling Technology), anti-Wnt5a (A12744, Thermo Scientific), and anti-Frizzled4 (FZD4) (A8161, Thermo Scientific). After three TBST washes, membranes were incubated for 1 h with HRP-conjugated goat anti-rabbit IgG (ab6721, Abcam), followed by additional washing to remove excess antibody. Protein bands were detected using an enhanced chemiluminescence substrate (B500024, Proteintech, Chicago, IL, USA). Images were captured with the Amersham Imager 600 system (General Electric Company, Boston, USA). Band intensities were quantified using Image-Pro Plus 6.2 (Media Cybernetics) and normalized to GAPDH. All assays were performed in at least three independent replicates.

Statistical analysis

Data distribution was evaluated using QQ plots; datasets aligning closely with a straight diagonal line were interpreted as approximately normally distributed. Quantitative variables are expressed as mean ± standard deviation (SD), and each experiment was independently repeated no fewer than three times. Differences among multiple groups were examined using one-way ANOVA, followed by the least significant difference (LSD) post hoc test for pairwise comparisons. Statistical analyses were conducted in SPSS 25.0, and significance was determined at $P < 0.05$.

Results and Discussion

ED-71 improves bone quantity and quality in mice with GIOP

Four-week micro-CT assessments revealed distinct bone structural differences across the experimental groups. In CON mice, the trabecular network appeared well-organized with moderate marrow cavity size, and the diaphyseal cortical bone exhibited normal thickness **(Figures 1Aa and 1Ad)**. In contrast, MPED mice showed markedly diminished and scattered trabeculae, enlarged marrow cavities, and pronounced thinning of the cortical bone **(Figures 1Ab and 1Ae)**. Treatment with ED-71 substantially ameliorated these abnormalities: MPED+ED-71 animals displayed restored trabecular mass, reduced medullary cavity size, and noticeable improvement in cortical bone thickness compared with MPED mice **(Figures 1Ac and 1Af)**.

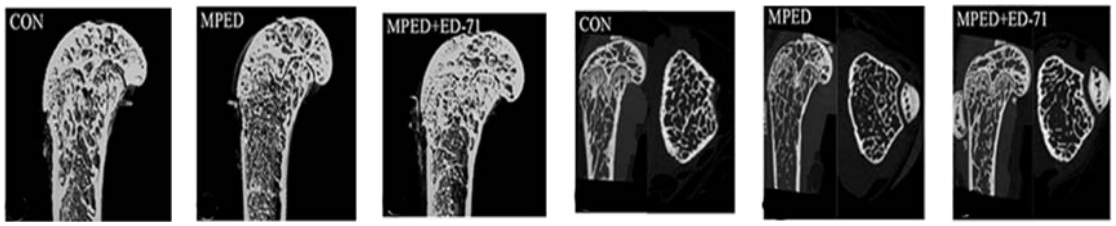

a) b) c) d) e) f)

A)

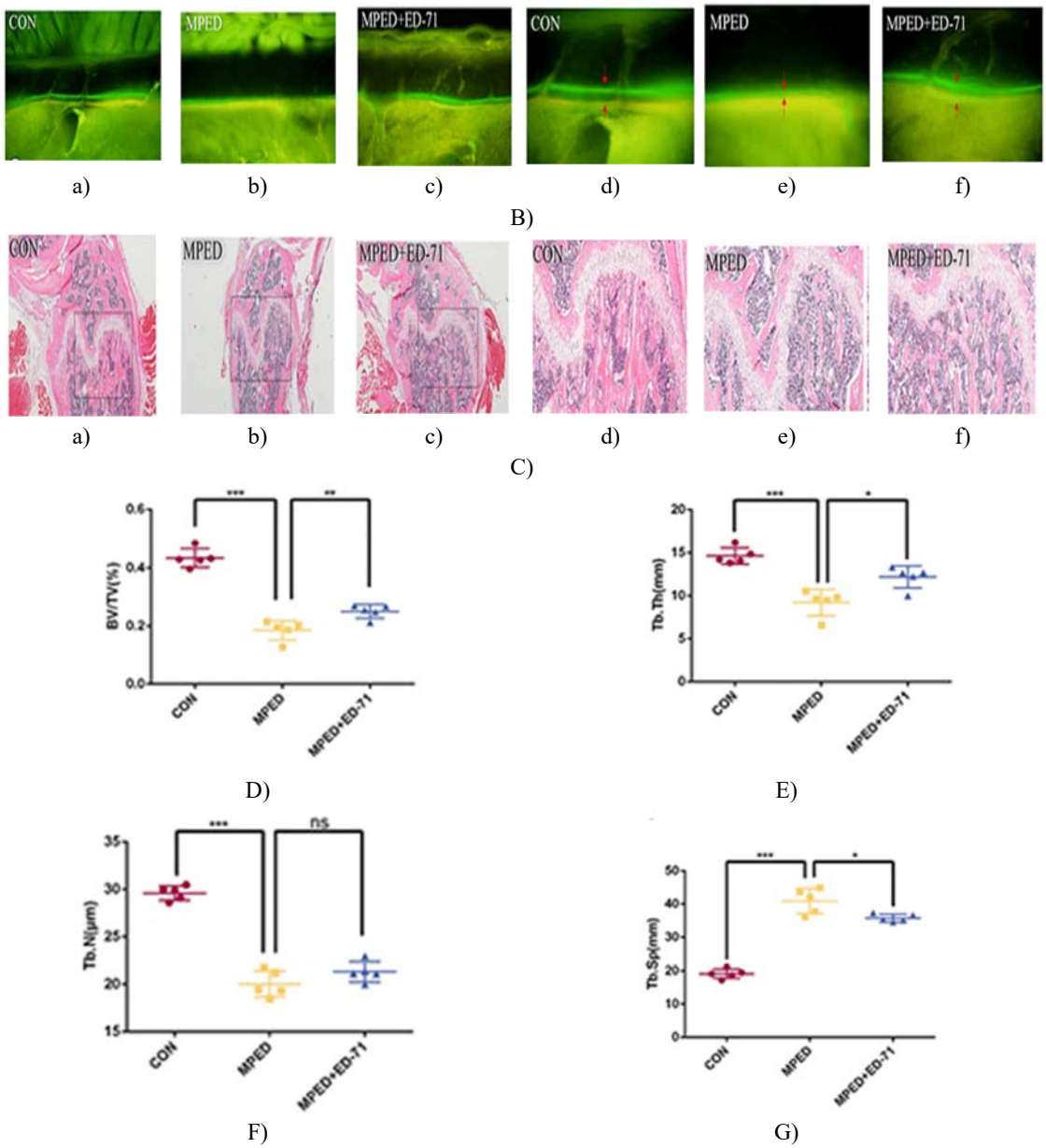

Figure 1. Effects of ED-71 on bone quantity and quality in MPED-induced osteoporosis mice. (A) a–f Representative 2D and 3D Micro-CT reconstructions of femoral bones from the CON, MPED, and MPED+ED-71 groups at week 4. (B) a–f Calcein and tetracycline double-labeling images of femurs at week 4; red arrows mark the separation between the two fluorochrome labels. Scale bars: 200 μm or 100 μm. (C) a–f HE-stained femoral sections. Scale bars: 1 mm or 500 μm. (D–G) Quantitative assessment of bone histological indicators. Error bars represent mean ± SD (n = 5). *P < 0.05, **P < 0.01, ***P < 0.001.
Abbreviations: ns, no significance; CON, control; MPED, methylprednisolone; MPED+ED-71, methylprednisolone+eldecalcitol; BV/TV, bone volume/tissue volume; Tb.N, trabeculae number; Tb.Th, trabeculae thickness; Tb.Sp, trabeculae separation.

In the CON group, HE-stained sections showed a dense and orderly trabecular framework with thick trabeculae and minimal spacing **(Figures 1Ca and 1Cd)**. This architecture was severely disrupted in MPED mice, where the cancellous bone region was markedly diminished, the trabeculae were loosely arranged, fewer in number, and widely separated **(Figures 1Cb and 1Ce)**. Administration of ED-71 substantially alleviated these steroid-induced alterations, resulting in increased cancellous bone mass, more robust and numerous trabeculae, and reduced trabecular spacing, effectively counteracting glucocorticoid-related bone deterioration **(Figures 1Cc and 1Cf)**.

Quantitative histology confirmed these observations: BV/TV was highest in CON mice, sharply reduced in MPED animals, and partially restored in MPED+ED-71 mice **(Figure 1D)**. A similar pattern was observed for trabecular number and thickness—both parameters were most preserved in CON mice, reached their lowest levels in MPED mice, and showed moderate improvement with ED-71 treatment. Although Tb.Th increased in MPED+ED-71 mice relative to MPED mice, the difference did not reach statistical significance **(Figures 1E and 1F)**. For Tb.Sp, CON animals displayed the smallest separation, MPED mice the most pronounced spacing, while MPED+ED-71 mice fell between these extremes **(Figure 1G)**.

Dynamic bone formation was evaluated using calcein/tetracycline double labeling. The distance between calcein (green) and tetracycline (yellow) marks the amount of newly formed bone over ten days. CON mice exhibited the largest spacing, indicative of rapid bone deposition **(Figures 1Ba and 1Bd)**. MPED mice demonstrated the smallest interval **(Figures 1Bb and 1Be)**, reflecting severely reduced formation rates. ED-71 treatment enhanced mineral apposition compared with MPED alone, showing a wider label separation and improved bone deposition dynamics **(Figures 1Bc and 1Bf)**.

Following eight weeks of DEX treatment, micro-CT results mirrored the patterns seen with MPED, although bone loss was even more pronounced **(Figures 2Aa–2Af)**. HE staining and related quantitative measurements also reflected greater reductions in cancellous bone structure and microarchitectural integrity. Additionally, unmineralized cartilage content decreased across groups at this later timepoint, and trabeculae appeared thinner in all conditions. The restorative effect of DEX+ED-71 on bone mass was more limited than that observed in MPED+ED-71 mice **(Figures 2Ca–2Cf and 2D–2G)**. The DEX group exhibited a stronger suppression of bone formation compared with MPED, while DEX+ED-71 partially rescued the formation rate, though still not to the level of the earlier timepoint **(Figures 2Ba–2Bf)**.

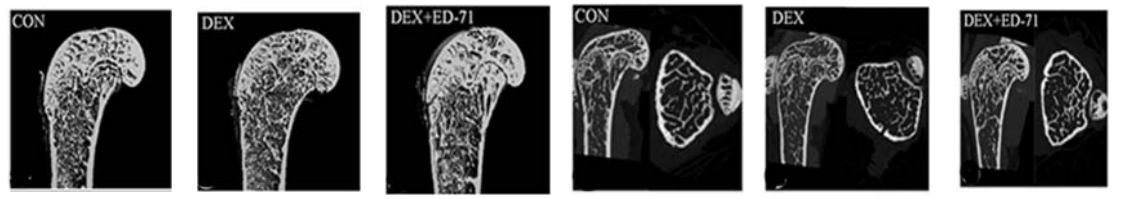

a) b) c) d) e) f)

A)

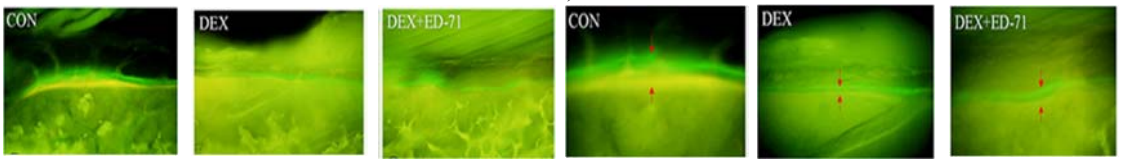

a) b) c) d) e) f)

B)

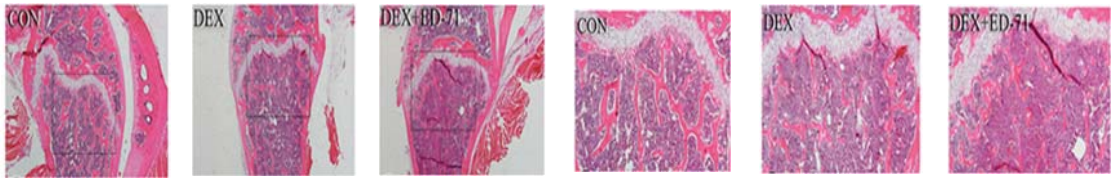

a) b) c) d) e) f)

C)

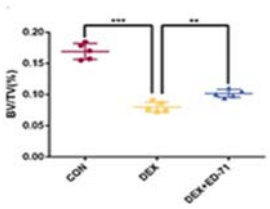

D)

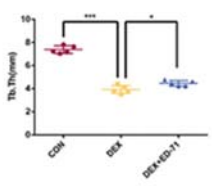

E)

F) G)

Figure 2. Influence of ED-71 on skeletal morphology in DEX-induced osteoporosis. (A) a–f display the 2D and 3D Micro-CT reconstructions of femurs from the CON, DEX, and DEX+ED-71 groups after 8 weeks. (B) a–f show calcein/tetracycline double-label images, with the red arrows marking the interval between the two fluorochromes. Scale bars: 200 μm or 100 μm. (C) a–f present HE-stained femoral sections (scale bars: 1 mm or 500 μm). (D–G) summarize the quantitative comparisons of histological bone parameters. Data are plotted as mean ± SD (n = 5). *P < 0.05, **P < 0.01, ***P < 0.001.

Abbreviations: CON, control; DEX, dexamethasone; DEX+ED-71, dexamethasone+eldecalcitol; BV/TV, bone volume/tissue volume; Tb.N, trabeculae number; Tb.Th, trabeculae thickness; Tb.Sp, trabeculae separation.

ED-71 promotes osteoblast activity and inhibits osteoclasts in GIOP mice

In untreated control mice, ALP-positive osteoblasts formed a continuous cell layer along the trabecular margins, while TRAP-positive osteoclasts appeared only sporadically **(Figures 3Aa and 3Ad)**. This pattern shifted dramatically in MPED-treated animals: osteoblast labeling was greatly diminished, and osteoclast staining also dropped compared with the CON group **(Figures 3Ab and 3Ae)**. Introducing ED-71 to MPED-treated mice reversed part of this suppression—ALP-positive osteoblast coverage increased noticeably, whereas TRAP-positive osteoclasts were even fewer than in both the CON and MPED groups **(Figures 3Ac and 3Af)**.

Quantitative evaluation reinforced these observations. ALP activity peaked in the CON mice, was sharply reduced following MPED treatment, and showed partial recovery with ED-71 administration. In contrast, the number of TRAP-marked osteoclasts followed a stepwise downward trend across all three groups, being lowest in MPED+ED-71 mice **(Figure 3B)**.

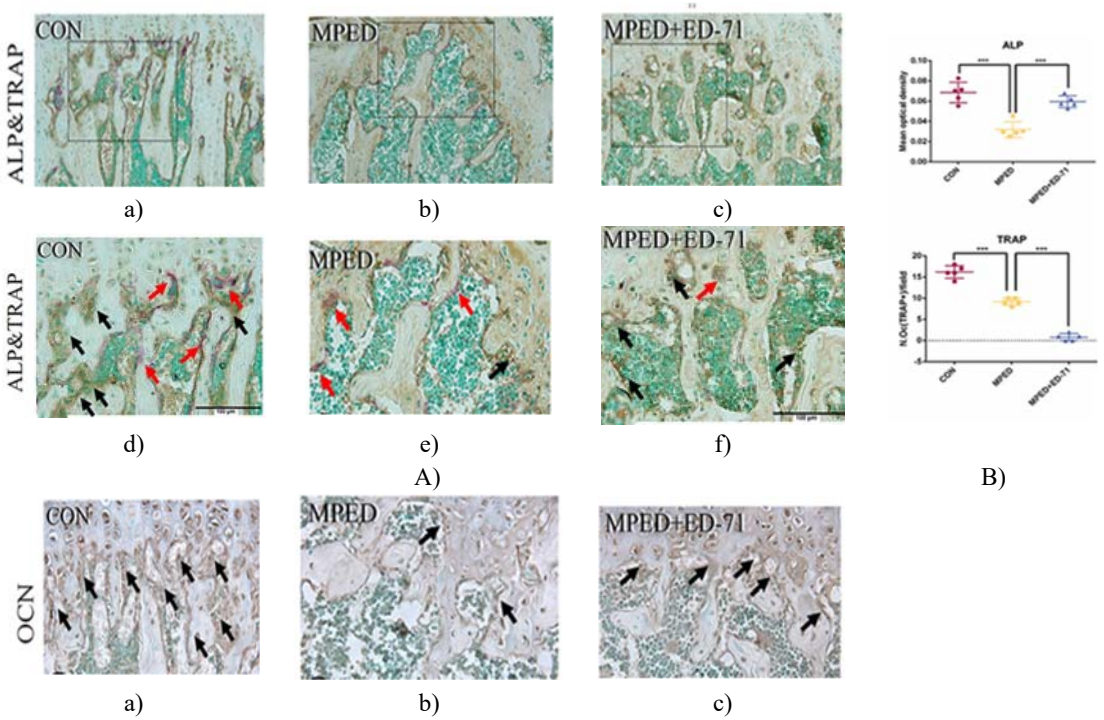

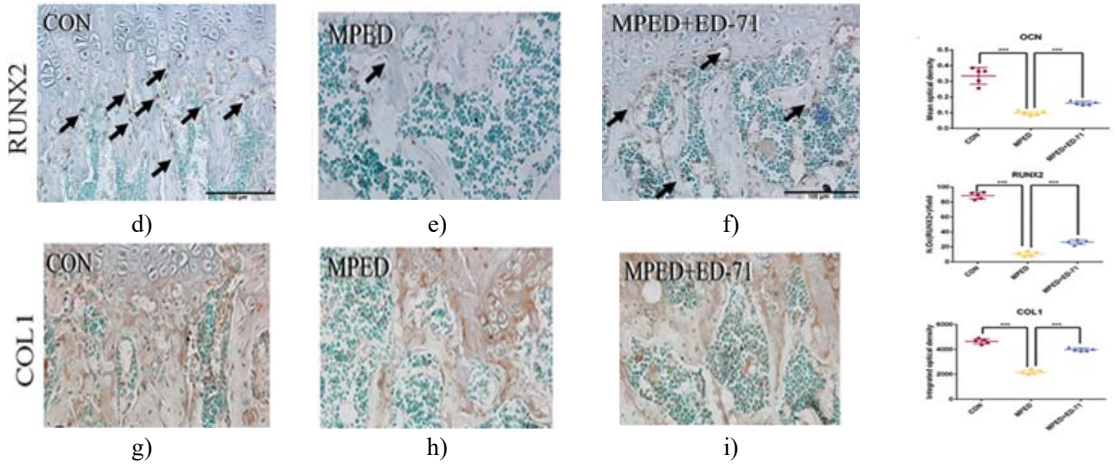

Figure 3. Effects of ED-71 on osteoblast and osteoclast activity in MPED-induced osteoporosis mice. (A) a–f ALP and TRAP double staining of femurs from CON, MPED, and MPED+ED-71 groups at week 4; black arrows indicate ALP-positive osteoblasts, and red arrows indicate TRAP-positive osteoclasts. Scale bars: 200 μm or 100 μm. (B) Quantification of ALP mean optical density and the number of TRAP-positive osteoclasts. (C) a–i Representative immunohistochemical staining for COL1, RUNX2, and OCN; black arrows indicate regions of positive expression. Scale bar: 100 μm. (D) Quantitative analysis of mean optical density for OCN, integrated optical density for COL1, and counts of RUNX2-positive osteoblasts. Data are expressed as mean ± SD (n = 5). ***P < 0.001.

In MPED-treated mice, COL1 and OCN expression levels were markedly lower than those in CON animals, accompanied by a reduction in RUNX2-positive osteoblasts **(Figures 3Ca, 3Cb, 3Cd, 3Ce, 3Cg and 3Ch)**. Administration of ED-71 partially restored these markers, with higher COL1 and OCN expression and an increased number of RUNX2-positive cells relative to the MPED group **(Figures 3Cc, 3Cf and 3Ci)**, a trend that was corroborated by statistical analysis **(Figure 3D).**

Eight-week DEX treatment produced a similar pattern: ALP-positive osteoblasts and TRAP-positive osteoclasts were both diminished compared with controls **(Figures 4Aa, 4Ab, 4Ad and 4Ae)**. In the DEX+ED-71 group, osteoblast activity increased while osteoclast numbers declined compared with DEX alone **(Figures 4Ac and 4Af)**, consistent with quantitative trends **(Figure 4B)**. Immunohistochemistry mirrored these observations: DEX reduced COL1 and OCN expression and decreased RUNX2-positive osteoblasts relative to CON mice **(Figures 4C a, 4Cb, 4Cd, 4Ce, 4Cg and 4Ch)**, whereas ED-71 co-treatment partially rescued these markers **(Figures 4C c, 4Cf and 4Ci)**. Statistical evaluation confirmed these patterns, though the recovery effect at eight weeks was less pronounced than at four weeks **(Figure 4D)**.

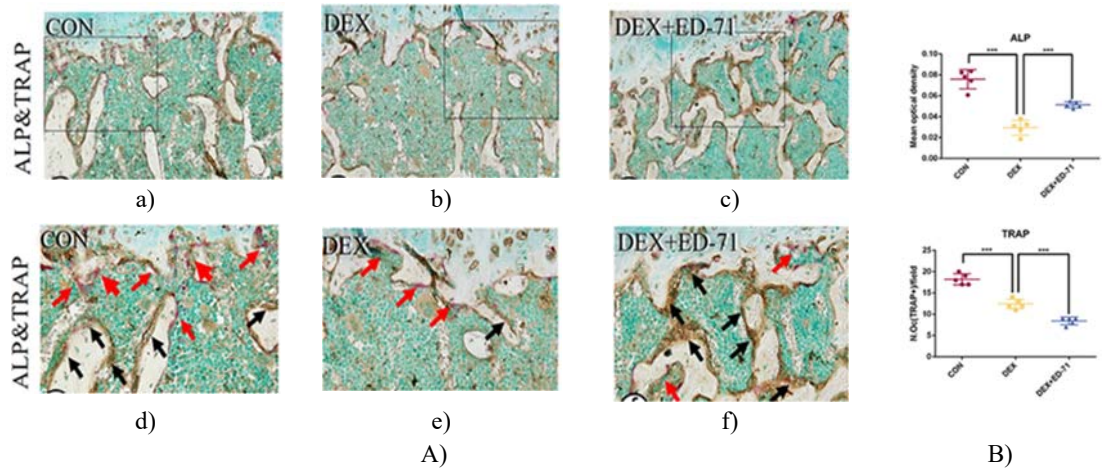

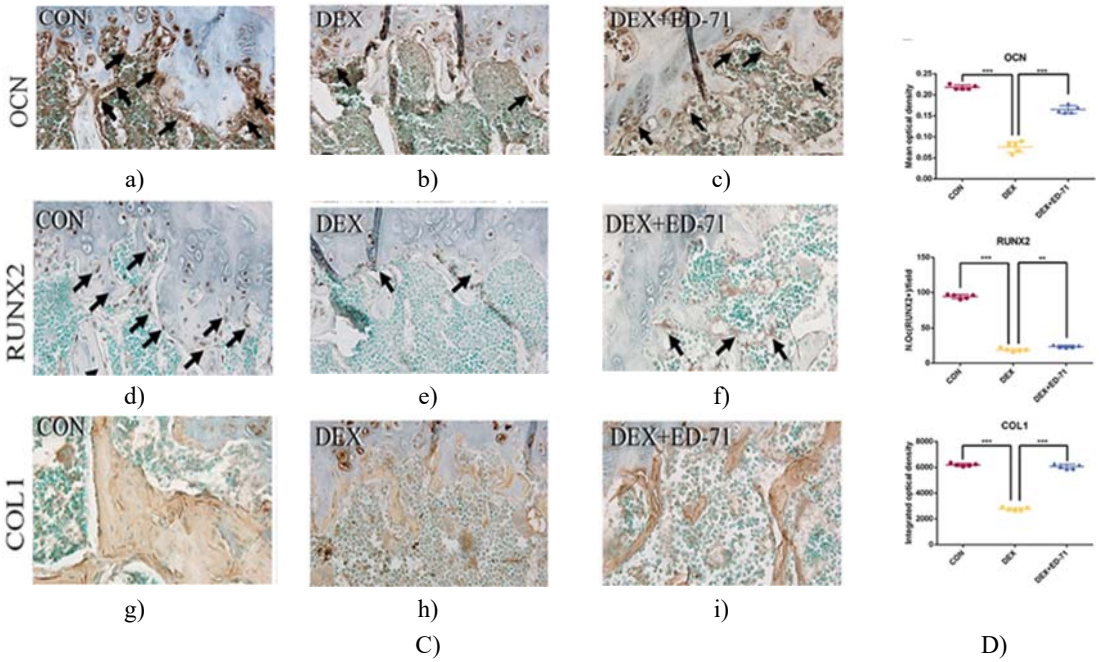

Figure 4. Effects of ED-71 on osteoblast and osteoclast activity in DEX-induced osteoporosis mice. (A) a–f ALP and TRAP double staining of femurs from CON, DEX, and DEX+ED-71 groups at week 8; black arrows indicate ALP-positive osteoblasts, red arrows indicate TRAP-positive osteoclasts. Scale bars: 200 μm or 100 μm. (B) Quantitative analysis of ALP mean optical density and TRAP-positive osteoclast numbers. (C) a–i Representative immunohistochemical staining for COL1, RUNX2, and OCN, with black arrows marking regions of positive expression. Scale bar: 100 μm. (D) Statistical evaluation of mean optical density of OCN, integrated optical density of COL1, and counts of RUNX2-positive osteoblasts. Data are presented as mean ± SD (n = 5). **P < 0.01, ***P < 0.001.

ED-71 Partially Reverses DEX-Induced Inhibition of MC3T3-E1 Osteoblast Differentiation and Mineralization

To investigate osteoblast function, ALP and Alizarin Red (AR) staining were performed at days 7 and 21 following treatment with DEX and ED-71. In the CON group, basal ALP activity was minimal, whereas osteoblast-inducing conditioned medium (OM group) markedly enhanced ALP expression. Exposure to DEX significantly suppressed ALP activity relative to the OM group. Notably, co-treatment with ED-71 partially rescued ALP activity in DEX-treated cells **(Figure 5a)**.

AR staining was used to evaluate calcium deposition, reflecting mineralization capacity. DEX treatment markedly reduced both AR staining intensity and the formation of mineralized nodules compared with untreated controls. Addition of ED-71 significantly increased mineralized nodule formation relative to DEX alone, indicating improved osteoblast mineralization **(Figure 5b)**.

Consistent with these findings, RT-qPCR analysis showed that ED-71 enhanced mRNA expression of osteogenic markers in MC3T3-E1 cells, including ALP, RUNX2, osterix (OSX), OCN, and COL1 **(Figure 5c)**. Western blot analysis confirmed that DEX treatment suppressed protein levels of ALP, RUNX2, COL1, and OCN, whereas ED-71 co-treatment partially restored these osteogenic proteins toward baseline levels (**Figures 5d and 5e)**.

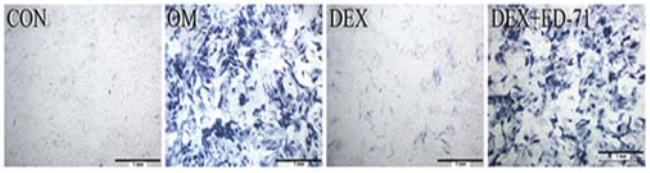

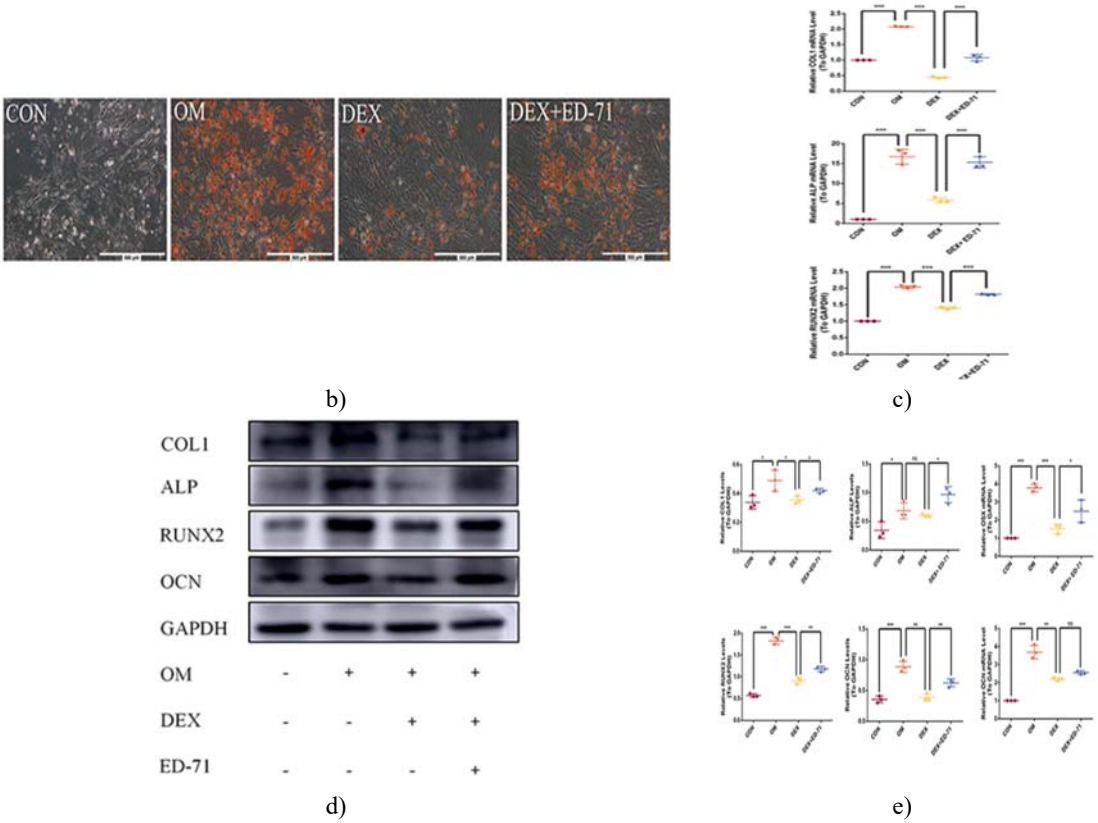

Figure 5. Effects of ED-71 on differentiation and mineralization of DEX-treated MC3T3-E1 cells. (a) ALP staining of MC3T3-E1 cells in the CON, OM, DEX, and DEX+ED-71 groups at day 7. Scale bar: 1 mm. (B) AR staining for calcium deposition in the same groups after 21 days of culture. Scale bar: 500 μm. (c) RT-qPCR analysis of COL1, ALP, RUNX2, OSX, and OCN mRNA levels after 7 days of induction, with GAPDH as an internal control. (d) Western blot detection of COL1, ALP, RUNX2, OCN, and GAPDH protein levels after 14 days. (e) Quantitative analysis of protein expression. Data represent mean ± SD from three independent experiments. *P < 0.05, **P < 0.01, ***P < 0.001.

Abbreviations: ns, no significance; CON, control; OM, osteoblast-inducing conditioned medium; DEX, dexamethasone; DEX+ED-71, dexamethasone+eldecalcitol.

ED-71 modulates notch and Wnt/GSK-3β/β-catenin signaling in DEX-inhibited MC3T3-E1 cells

To explore the molecular mechanisms underlying ED-71-mediated osteoblast differentiation, immunofluorescence was employed to examine the Notch and Wnt/GSK-3β/β-catenin pathways. In the OM group, β-catenin levels were markedly increased in both the cytoplasm and nucleus compared with the CON group. DEX treatment significantly suppressed β-catenin expression, whereas ED-71 co-treatment partially restored its nuclear and cytoplasmic localization **(Figure 6a)**, consistent with the notion that ED-71 promotes osteogenesis via activation of Wnt/GSK-3β/β-catenin signaling.

Regarding Notch signaling, Notch1 fluorescence was reduced in OM cells compared with CON, while DEX exposure elevated Notch1 signal. Addition of ED-71 counteracted this effect, lowering Notch1 fluorescence relative to the DEX group **(Figure 6b)**. RT-qPCR analysis corroborated these findings: OM conditions increased β-catenin mRNA and decreased Notch1 mRNA compared with CON, whereas DEX reversed these trends. ED-71 treatment partially normalized the expression of both genes toward OM levels **(Figure 6c)**.

Western blot results aligned with these observations: OM cells exhibited higher β-catenin and lower Notch1 protein levels. DEX reduced GSK-3β, total β-catenin, active β-catenin, Wnt5a, and FZD4, while elevating Notch1. In contrast, co-treatment with ED-71 restored the Wnt/GSK-3β/β-catenin components and partially suppressed Notch1 expression, demonstrating that ED-71 can mitigate DEX-induced suppression of osteogenic signaling **(Figures 6d and 6e)**.

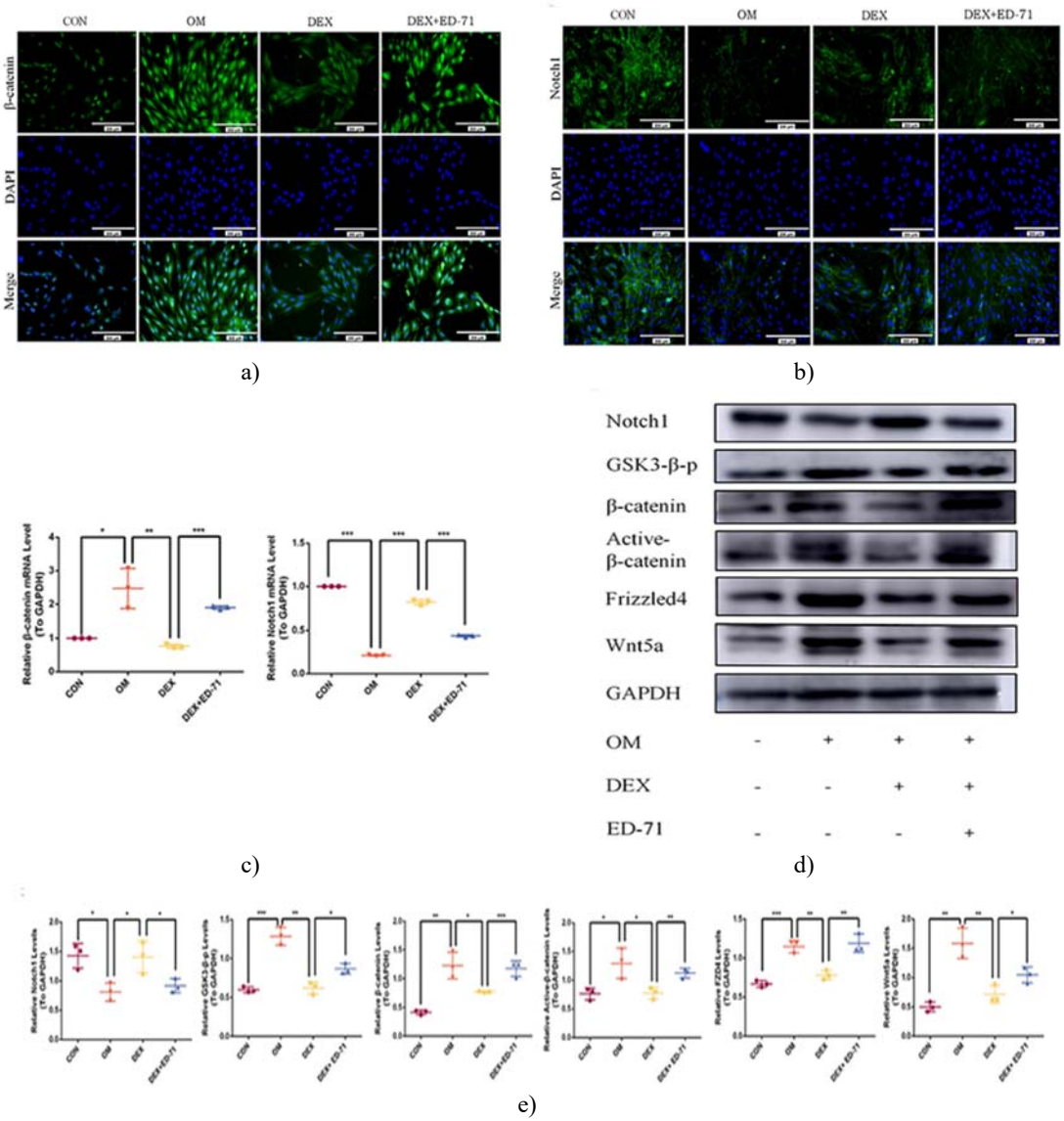

Figure 6. ED-71 modulates MC3T3-E1 cells via Notch and Wnt/GSK-3β/β-catenin signaling. (A) Representative immunofluorescence images showing β-catenin localization in CON, OM, DEX, and DEX+ED-71 groups at day 7. Scale bar: 200 μm. (B) Immunofluorescence staining of Notch1 in the same groups at day 7. Scale bar: 200 μm. (C) RT-qPCR analysis of β-catenin and Notch1 mRNA levels after 7 days, with GAPDH as internal control. (D) Western blot detection of Wnt5a, FZD4, active β-catenin, total β-catenin, phosphorylated GSK-3β, Notch1, and GAPDH after 14 days. (E) Quantitative analysis of Western blot data. Values represent mean ± SD from three independent experiments. *P < 0.05, **P < 0.01, ***P < 0.001.

Abbreviations: CON, control; OM, osteoblast-inducing conditioned medium; DEX, dexamethasone; DEX+ED-71, dexamethasone+eldecalcitol.

Wnt signaling inhibition by XAV939 attenuates ED-71 effects

To further confirm the role of Wnt/β-catenin signaling in ED-71-mediated osteogenesis, MC3T3-E1 cells were treated with the Wnt pathway inhibitor XAV939. In the presence of DEX, co-treatment with XAV939 significantly suppressed ALP activity and reduced mineralized nodule formation compared with DEX alone **(Figures 7a and 7b)**. In addition, XAV939 markedly lowered mRNA levels of COL1, ALP, RUNX2, and OCN **(Figure 7c)** and decreased protein expression of RUNX2, OCN, active β-catenin, Wnt5a, and FZD4 **(Figures 7d,**

and 7e). These results indicate that Wnt/β-catenin signaling is critical for the differentiation and mineralization of MC3T3-E1 osteoblasts and mediates, at least in part, the pro-osteogenic effects of ED-71.

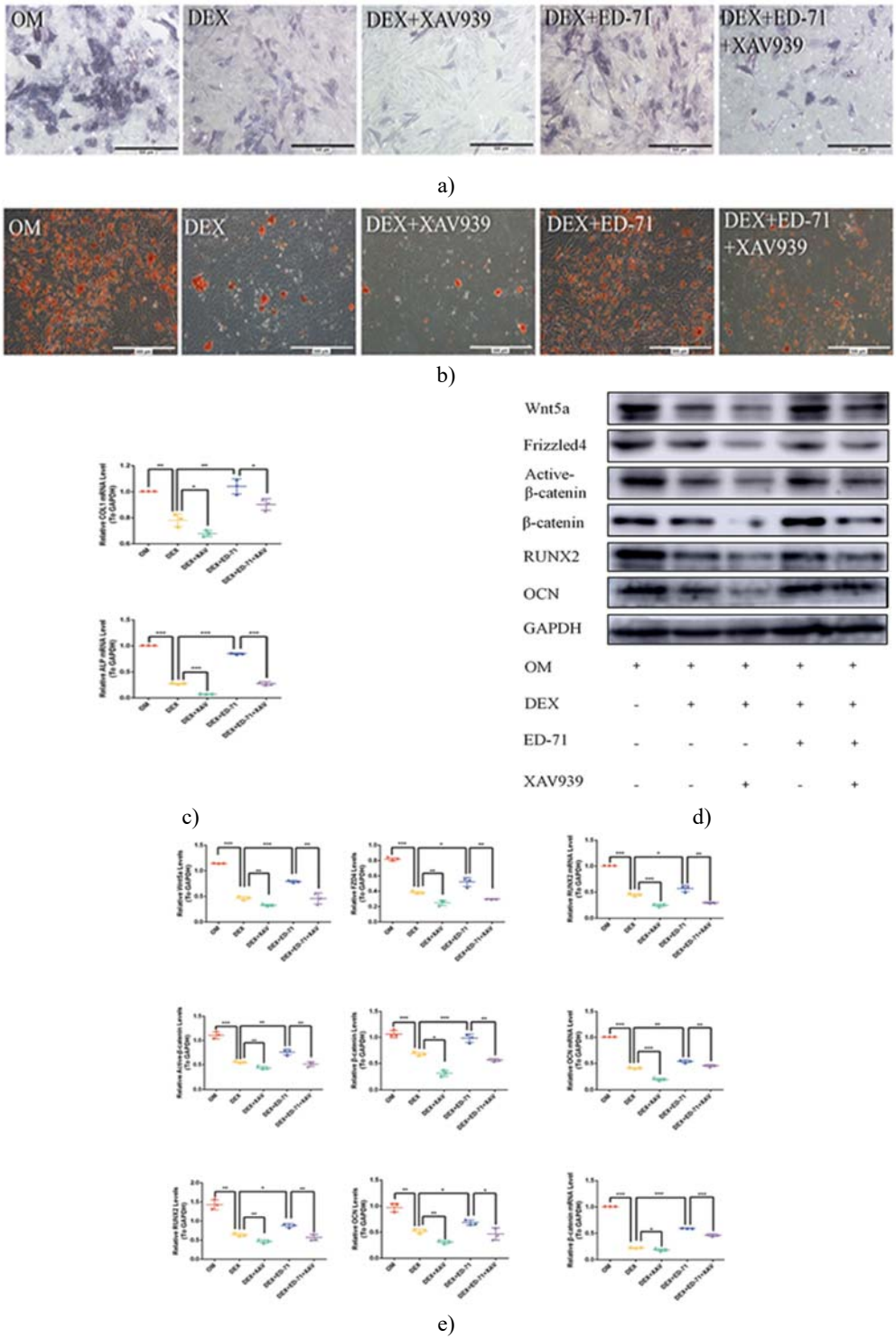

Figure 7. The Wnt pathway inhibitor XAV939 attenuates the effects of ED-71. (A) ALP staining of MC3T3-E1 cells in OM, DEX, DEX+XAV939, DEX+ED-71, and DEX+ED-71+XAV939 groups at day 7. Scale bar: 500 μm. (B) AR staining of mineralized nodules in the same groups after 21 days of culture. Scale bar: 500 μm. (C) RT-qPCR analysis of COL1, ALP, RUNX2, OCN, and β-catenin mRNA levels after 7 days, with GAPDH as internal control. (D) Western blot detection of β-catenin, RUNX2, OCN, Wnt5a, active β-catenin,

FZD4, and GAPDH after 14 days. (E) Quantitative analysis of protein expression. Data are presented as mean ± SD from three independent experiments. *P < 0.05, **P < 0.01, ***P < 0.001.
Abbreviations: OM, osteoblast-inducing conditioned medium; DEX, dexamethasone; DEX+XAV939, dexamethasone+XAV939; DEX+ED-71, dexamethasone+eldecalcitol; DEX+ED-71+XAV939, dexamethasone+eldecalcitol+XAV939.

ALP activity and formation of mineralized nodules in the DEX+ED-71+XAV939 group were reduced compared with DEX+ED-71 alone, yet remained higher than in the DEX+XAV939 group **(Figures 7a and 7b)**. Similarly, mRNA levels of COL1, ALP, RUNX2, and OCN were lowered by XAV939 in the DEX+ED-71+XAV939 group **(Figure 7c)**, and protein levels of RUNX2, OCN, active β-catenin, Wnt5a, and FZD4 were also decreased **(Figures 7d and 7e)**, though they were still above those observed in DEX+XAV939 cells. These results indicate that XAV939 partially antagonized the protective effects of ED-71, confirming that its pro-osteogenic action depends on Wnt/β-catenin signaling in DEX-inhibited MC3T3-E1 cells.

Notch1 overexpression partially reverses ED-71 effects

Hes1 overexpression reduced ALP activity and mineralized nodule formation compared with DEX+ED-71-treated cells **(Figures 8a and 8b)**. Additionally, Hes1 upregulation decreased mRNA expression of COL1, ALP, RUNX2, and OCN **(Figures 8c)**, as well as protein levels of RUNX2 and OCN **(Figures 8d and 8c)**. These findings suggest that activation of Notch signaling negatively regulates MC3T3-E1 differentiation and mineralization, partially counteracting the osteogenic effects of ED-71.

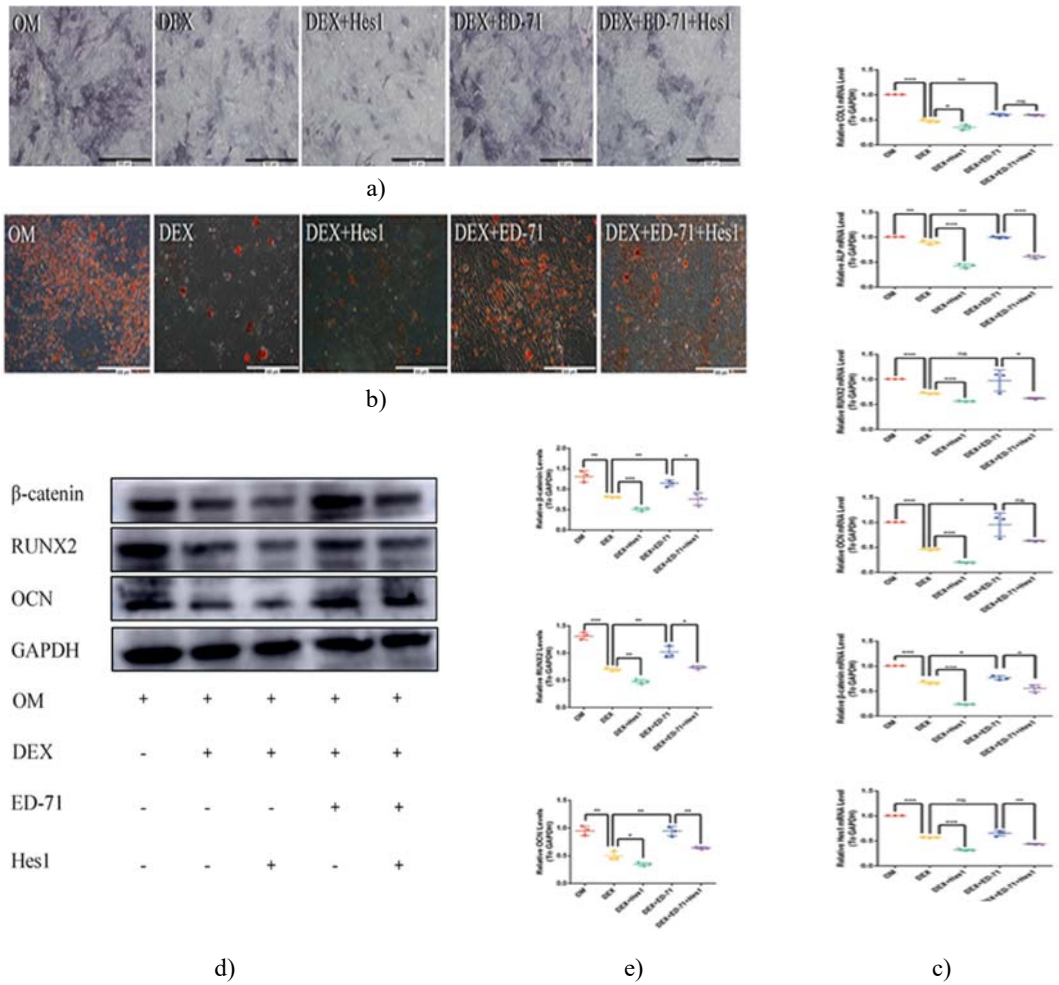

Figure 8. Notch1 overexpression attenuates ED-71-induced osteogenesis. (a) ALP staining of MC3T3-E1 cells in OM, DEX, DEX+Hes1, DEX+ED-71, and DEX+ED-71+Hes1 groups at day 7. Scale bar: 500 μm.

(b) AR staining of mineralized nodules in the same groups after 21 days. Scale bar: 500 μm. (c) RT-qPCR analysis of COL1, ALP, RUNX2, OCN, β-catenin, and Hes1 mRNA after 7 days, with GAPDH as an internal control. (d) Western blot detection of β-catenin, RUNX2, OCN, and GAPDH after 14 days. (e) Quantitative analysis of protein expression. Data represent mean ± SD from three independent experiments. *P < 0.05, **P < 0.01, ***P < 0.001.

Abbreviations: ns, no significance; OM, osteoblast-inducing conditioned medium; DEX, dexamethasone; DEX+Hes1, dexamethasone+Hes1 transfection; DEX+ED-71, dexamethasone+eldecalcitol; DEX+ED-71+Hes1, dexamethasone+eldecalcitol+Hes1 transfection.

Overexpression of Hes1 led to a reduction in both ALP activity and mineralized nodule formation in the DEX+ED-71+Hes1 group compared with DEX+ED-71-treated cells, although these values remained higher than those in the DEX+Hes1 group **(Figures 8a and 8b).** Similarly, mRNA expression of COL1, ALP, RUNX2, and OCN **(Figure 8c)** and protein levels of RUNX2 and OCN **(Figures 8d and 8e)** were decreased in the DEX+ED-71+Hes1 group relative to DEX+ED-71, yet still above DEX+Hes1 alone. Notably, both β-catenin mRNA and protein levels declined following Notch activation **(Figures 8c–8e)**, indicating that Hes1-mediated Notch signaling negatively influences Wnt/β-catenin activity and partially reverses the pro-osteogenic effects of ED-71.

Discussion

This study investigated the protective role of ED-71 against glucocorticoid-induced osteoporosis (GIOP) and evaluated its capacity to enhance osteoblast differentiation under glucocorticoid stress. Our findings demonstrate that ED-71 mitigates GIOP by improving bone mass, microarchitecture, and dynamic formation rates, primarily through promotion of osteoblast activity. Mechanistically, ED-71 appears to exert its osteogenic effects by simultaneously suppressing Notch signaling and stimulating the Wnt/GSK-3β/β-catenin pathway **(Figure 9)**, thereby facilitating osteoblast differentiation and counteracting glucocorticoid-induced inhibition.

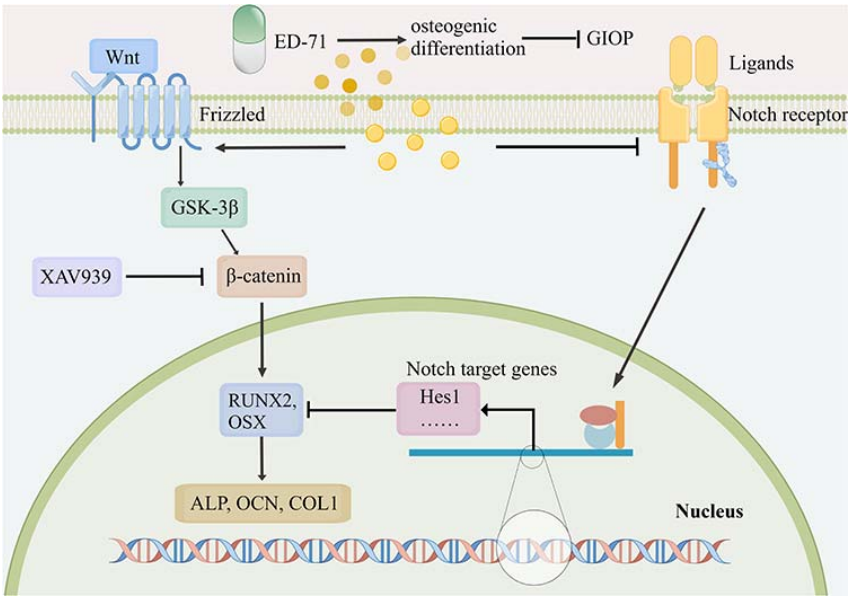

Figure 9. Schematic illustration of ED-71-mediated prevention of GIOP through regulation of osteogenic differentiation via Notch and Wnt/GSK-3β/β-catenin signaling. ED-71 prevented GIOP by enhancing bone mass, bone quality, and bone formation rates. Mechanistically, ED-71 may exert its effects by suppressing Notch signaling while activating Wnt/GSK-3β/β-catenin signaling (Figdraw, www.figdraw.com).

Chronic or high-dose glucocorticoid therapy often leads to the iatrogenic condition, GIOP [2]. In this study, two commonly used glucocorticoids—methylprednisolone (MPED) and dexamethasone (DEX)—were employed to establish a murine GIOP model and assess glucocorticoid-induced bone impairment comprehensively [33, 34]. MPED and DEX are classified as short-acting (half-life 12–36 hours) and long-acting (half-life 36–72 hours) glucocorticoids, respectively [35]. Micro-CT, HE staining, and calcein/tetracycline double labeling of the

proximal femur demonstrated that MPED or DEX treatment decreased new bone formation, thinned cortical bone, reduced BV/TV, decreased trabecular number and thickness, and increased trabecular separation. These findings are consistent with previously reported glucocorticoid-mediated bone deterioration in GIOP [36]. Notably, ED-71 treatment markedly mitigated these deleterious effects, preserving bone mass and microarchitecture, in line with prior clinical and experimental studies [37, 38]. Moreover, ED-71 showed efficacy in models without prior glucocorticoid exposure [39], supporting its potential as a preventive therapy for primary GIOP.

Focusing on osteoblast and osteoclast activity, ALP serves as a key marker of osteoblast differentiation and bone formation [40, 41], RUNX2 regulates osteoblast maturation and mineralization [42], OCN indicates late-stage osteoblast differentiation [43], and COL1 marks advanced osteogenesis [44]. In vivo immunohistochemistry revealed reduced expression of ALP, RUNX2, OCN, and COL1 in GIOP femurs, while ED-71 administration significantly restored these markers. Parallel in vitro experiments showed that ED-71 counteracted DEX-mediated inhibition of MC3T3-E1 cell differentiation and mineralization. Previous studies on ED-71's effects on osteoblasts have been inconsistent: some demonstrated promotion of pre-osteoblast differentiation without affecting proliferation [16, 45], enhancement of osteoblast differentiation under osteoclast-mediated bone resorption [46], or protective effects in diabetic osteoporosis [17], whereas others reported inhibitory effects in vitro [46, 47]. These discrepancies may stem from differences in experimental conditions, with our study being the first to assess ED-71 effects on osteoblasts under glucocorticoid-induced stress.

TRAP staining was used to evaluate osteoclasts [48]. Interestingly, MPED and DEX did not increase TRAP-positive cells as previously reported [32], suggesting stage-dependent glucocorticoid effects on osteoclasts [2]. ED-71 treatment suppressed osteoclast activity, consistent with prior findings [16, 48], likely through modulation of RANKL/OPG ratio, EphrinB2–EphB4 signaling, and sphingosine-1-phosphate (S1P) pathways [14, 19, 49]. Further mechanistic studies are warranted to clarify how ED-71 inhibits osteoclast-mediated bone resorption in GIOP.

Regarding signaling pathways, ED-71 promoted osteogenic differentiation by suppressing Notch signaling and activating Wnt/GSK-3β/β-catenin signaling. Wnt5a binding to FZD4 positively regulates osteogenesis [50, 51], and ED-71 treatment restored downstream regulators perturbed by glucocorticoids. Blocking Wnt signaling with XAV939 partially abrogated ED-71-induced osteoblast differentiation and mineralization [52]. Conversely, Notch pathway activation via Hes1 overexpression inhibited ED-71-mediated osteogenesis and reduced β-catenin expression, indicating crosstalk between Notch and Wnt/β-catenin pathways. Glucocorticoids are known to suppress Wnt signaling in osteoblasts [53], and Wnt inhibition has been shown to prevent GIOP progression [54]. Notch signaling negatively regulates osteoblast differentiation and contributes to osteopenia [55], highlighting the importance of low Notch activity in early osteoblast development. GSK-3β may mediate interactions between Notch and Wnt pathways [56–58]. Together, these findings support the conclusion that ED-71 exerts protective effects in GIOP by coordinating Notch and Wnt/GSK-3β/β-catenin signaling.

Nevertheless, this study has limitations, including restricted time points for observation. Future investigations should incorporate broader temporal analyses. Furthermore, ED-71 only partially counteracts glucocorticoid-induced bone loss, suggesting that combination therapy with other agents may enhance outcomes. Simultaneous ED-71 supplementation during glucocorticoid exposure also warrants further study to determine its potential in reversing established GIOP.

Conclusion

In summary, our results provide strong evidence that ED-71 effectively prevents GIOP progression by promoting osteoblast differentiation. This effect involves inhibition of Notch signaling and activation of Wnt/GSK-3β/β-catenin pathways, underscoring the potential of ED-71 as a clinically valuable therapeutic option for GIOP and a promising candidate for future drug development.

Acknowledgments: None

Conflict of Interest: None

Financial Support: None

Ethics Statement: None

References

1. Compston J. Glucocorticoid-induced osteoporosis: an update. Endocrine. 2018;61(1):7-16. doi:10.1007/s12020-018-1588-2
2. Chotiyarnwong P, McCloskey EV. Pathogenesis of glucocorticoid-induced osteoporosis and options for treatment. Nat Rev Endocrinol. 2020;16(8):437-47. doi:10.1038/s41574-020-0341-0
3. Peng CH, Lin WY, Yeh KT, Chen IH, Wu WT, Lin MD. The molecular etiology and treatment of glucocorticoid-induced osteoporosis. Tzu Chi Med J. 2021;33(3):212-23. doi:10.4103/tcmj.tcmj_233_20
4. Chiodini I, Merlotti D, Falchetti A, Gennari L. Treatment options for glucocorticoid-induced osteoporosis. Expert Opin Pharmacother. 2020;21(6):721-32. doi:10.1080/14656566.2020.1721467
5. Cheng CH, Chen LR, Chen KH. Osteoporosis due to hormone imbalance: an overview of the effects of estrogen deficiency and glucocorticoid overuse on bone turnover. Int J Mol Sci. 2022;23(3):1376. doi:10.3390/ijms23031376
6. Han Y, Zhang L, Xing Y, Wu Z, Fu X, Zhao X, et al. Autophagy relieves the function inhibition and apoptosis-promoting effects on osteoblast induced by glucocorticoid. Int J Mol Med. 2018;41(2):800-8. doi:10.3892/ijmm.2017.3270
7. Gado M, Baschant U, Hofbauer LC, Henneicke H. Bad to the bone: the effects of therapeutic glucocorticoids on osteoblasts and osteocytes. Front Endocrinol (Lausanne). 2022;13:835720. doi:10.3389/fendo.2022.835720
8. Kobza AO, Herman D, Papaioannou A. Understanding and managing corticosteroid-induced osteoporosis. Open Access Rheumatol. 2021;13:177-90.
9. Leipe J, Holle JU, Weseloh C, Pfeil A, Krüger K. German Society of Rheumatology recommendations for management of glucocorticoid-induced osteoporosis. Z Rheumatol. 2021;80(Suppl 2):49-63. doi:10.1007/s00393-021-01025-z
10. Christakos S, Dhawan P, Verstuyf A, Verlinden L, Carmeliet G. Vitamin D: metabolism, molecular mechanism of action, and pleiotropic effects. Physiol Rev. 2016;96(1):365-408. doi:10.1152/physrev.00014.2015
11. Saito K, Miyakoshi N, Matsunaga T, Hongo M, Kasukawa Y, Shimada Y. Eldecalcitol improves muscle strength and dynamic balance in postmenopausal women with osteoporosis: an open-label randomized controlled study. J Bone Miner Metab. 2016;34(5):547-54. doi:10.1007/s00774-015-0695-x
12. Shintani T, Rosli SNZ, Takatsu F, Choon LY, Yamane S, Umezawa K, et al. Eldecalcitol (ED-71), an analog of 1α,25-dihydroxyvitamin D3 as a potential anti-cancer agent for oral squamous cell carcinomas. J Steroid Biochem Mol Biol. 2016;164:79-84. doi:10.1016/j.jsbmb.2015.09.043
13. Liu H, Wang G, Wu T, Mu Y, Gu W. Efficacy and safety of eldecalcitol for osteoporosis: a meta-analysis of randomized controlled trials. Front Endocrinol (Lausanne). 2022;13:854439. doi:10.3389/fendo.2022.854439
14. Zhang Y, Kou Y, Yang P, Zhang J, Chen H, Liu X, et al. ED-71 inhibited osteoclastogenesis by enhancing EphrinB2-EphB4 signaling between osteoclasts and osteoblasts in osteoporosis. Cell Signal. 2022;96:110376. doi:10.1016/j.cellsig.2022.110376
15. Takeda S, Saito M, Sakai S, Yogo K, Marumo K, Endo K. Eldecalcitol, an active vitamin D(3) derivative, prevents trabecular bone loss and bone fragility in type I diabetic model rats. Calcif Tissue Int. 2017;101(4):433-44. doi:10.1007/s00223-017-0298-8
16. de Freitas PH, Hasegawa T, Takeda S, Sasaki M, Saito H, Mori H, et al. Eldecalcitol, a second-generation vitamin D analog, drives bone minimodeling and reduces osteoclastic number in trabecular bone of ovariectomized rats. Bone. 2011;49(3):335-42. doi:10.1016/j.bone.2011.05.022
17. Lu Y, Liu S, Yang P, Kou Y, Li C, Liu H, et al. Exendin-4 and eldecalcitol synergistically promote osteogenic differentiation of bone marrow mesenchymal stem cells through M2 macrophages polarization via PI3K/AKT pathway. Stem Cell Res Ther. 2022;13(1):113. doi:10.1186/s13287-022-02800-8
18. Wang W, Gao Y, Liu H, Zhang Y, Ma Y, Zhao L, et al. Eldecalcitol, an active vitamin D analog, effectively prevents cyclophosphamide-induced osteoporosis in rats. Exp Ther Med. 2019;18(3):1571-80. doi:10.3892/etm.2019.7759

19. Han X, Du J, Liu D, Liu H, Amizuka N, Li M. Histochemical examination of systemic administration of eldecalcitol combined with guided bone regeneration for bone defect restoration in rats. J Mol Histol. 2017;48(1):41-51. doi:10.1007/s10735-016-9705-0
20. Matsumoto T, Yamamoto K, Takeuchi T, Tanaka Y, Tanaka S, Nakano T, et al. Eldecalcitol is superior to alfacalcidol in maintaining bone mineral density in glucocorticoid-induced osteoporosis patients (e-GLORIA). J Bone Miner Metab. 2020;38(4):522-32. doi:10.1007/s00774-020-01091-4
21. Zanotti S, Smerdel-Ramoya A, Canalis E. HES1 (hairy and enhancer of split 1) is a determinant of bone mass. J Biol Chem. 2011;286(4):2648-57. doi:10.1074/jbc.M110.183038
22. Lee SY, Long F. Notch signaling suppresses glucose metabolism in mesenchymal progenitors to restrict osteoblast differentiation. J Clin Invest. 2018;128(12):5573-86. doi:10.1172/JCI96221
23. Xu Y, Li L, Tang Y, Yang J, Jin Y, Ma C. Icariin promotes osteogenic differentiation by suppressing Notch signaling. Eur J Pharmacol. 2019;865:172794. doi:10.1016/j.ejphar.2019.172794
24. Pereira RM, Delany AM, Durant D, Canalis E. Cortisol regulates the expression of Notch in osteoblasts. J Cell Biochem. 2002;85(2):252-8. doi:10.1002/jcb.10125
25. Baron R, Gori F. Targeting WNT signaling in the treatment of osteoporosis. Curr Opin Pharmacol. 2018;40:134-41. doi:10.1016/j.coph.2018.04.011
26. Zhang Y, Wang Y, Zheng G, Liu Y, Li J, Huang H, et al. Follistatin-like 1 (FSTL1) interacts with Wnt ligands and Frizzled receptors to enhance Wnt/β-catenin signaling in obstructed kidneys in vivo. J Biol Chem. 2022;298(7):102010. doi:10.1016/j.jbc.2022.102010
27. Pan FF, Shao J, Shi CJ, Li ZP, Fu WM, Zhang JF. Apigenin promotes osteogenic differentiation of mesenchymal stem cells and accelerates bone fracture healing via activating Wnt/β-catenin signaling. Am J Physiol Endocrinol Metab. 2021;320(4):E760-71. doi:10.1152/ajpendo.00543.2019
28. Karsenty G, Olson EN. Bone and muscle endocrine functions: unexpected paradigms of inter-organ communication. Cell. 2016;164(6):1248-56. doi:10.1016/j.cell.2016.02.043
29. Ye YC, Zhao JL, Lu YT, Gao W, Zhao Y, Wang X, et al. Notch signaling via WNT regulates the proliferation of alternative, CCR2-independent tumor-associated macrophages in hepatocellular carcinoma. Cancer Res. 2019;79(16):4160-72. doi:10.1158/0008-5472.CAN-18-1691
30. Wu D, Pan W. GSK3: a multifaceted kinase in Wnt signaling. Trends Biochem Sci. 2010;35(3):161-8. doi:10.1016/j.tibs.2009.10.002
31. Shao J, Zhou Y, Xiao Y. The regulatory roles of Notch in osteocyte differentiation via the crosstalk with canonical Wnt pathways during the transition of osteoblasts to osteocytes. Bone. 2018;108:165-78. doi:10.1016/j.bone.2018.01.010
32. Wang Y, Chen J, Chen J, Liao Z, Qiu J, Yang Z, et al. Daphnetin ameliorates glucocorticoid-induced osteoporosis via activation of Wnt/GSK-3β/β-catenin signaling. Toxicol Appl Pharmacol. 2020;409:115333. doi:10.1016/j.taap.2020.115333
33. Lian WS, Ko JY, Chen YS, Ke HJ, Hsieh CK, Kuo CW, et al. Chaperonin 60 sustains osteoblast autophagy and counteracts glucocorticoid aggravation of osteoporosis by chaperoning RPTOR. Cell Death Dis. 2018;9(10):938. doi:10.1038/s41419-018-0970-6
34. Lin NY, Chen CW, Kagwiria R, Liang CY, Lin FH, Wu JJ, et al. Inactivation of autophagy ameliorates glucocorticoid-induced and ovariectomy-induced bone loss. Ann Rheum Dis. 2016;75(6):1203-10. doi:10.1136/annrheumdis-2015-207240
35. Hemani SA, Glover B, Ball S, Harrison A, Szefler SJ, Cicutto L, et al. Dexamethasone versus prednisone in children hospitalized for acute asthma exacerbations. Hosp Pediatr. 2021;11(11):1263-72. doi:10.1542/hpeds.2020-004788
36. Briot K, Roux C. Glucocorticoid-induced osteoporosis. RMD Open. 2015;1(1):e000014. doi:10.1136/rmdopen-2014-000014
37. Tanaka Y, Nakamura T, Nishida S, Suzuki K, Takeda S, Sato K, et al. Effects of a synthetic vitamin D analog, ED-71, on bone dynamics and strength in cancellous and cortical bone in prednisolone-treated rats. J Bone Miner Res. 1996;11(3):325-36. doi:10.1002/jbmr.5650110306
38. Kinoshita H, Miyakoshi N, Kasukawa Y, Sakai S, Shiraishi A, Segawa T, et al. Effects of eldecalcitol on bone and skeletal muscles in glucocorticoid-treated rats. J Bone Miner Metab. 2016;34(2):171-8. doi:10.1007/s00774-015-0664-4

39. Nakamura T, Takano T, Fukunaga M, Shiraki M, Matsumoto T. Eldecalcitol is more effective for the prevention of osteoporotic fractures than alfacalcidol. J Bone Miner Metab. 2013;31(4):417-22. doi:10.1007/s00774-012-0418-5
40. Yang L, Yang J, Pan T, Zhong X. Liraglutide increases bone formation and inhibits bone resorption in rats with glucocorticoid-induced osteoporosis. J Endocrinol Invest. 2019;42(9):1125-31. doi:10.1007/s40618-019-01034-5
41. Vimalraj S. Alkaline phosphatase: structure, expression and its function in bone mineralization. Gene. 2020;754:144855. doi:10.1016/j.gene.2020.144855
42. Hou Z, Wang Z, Tao Y, Bai J, Yu B, Shen J, et al. KLF2 regulates osteoblast differentiation by targeting of Runx2. Lab Invest. 2019;99(2):271-80. doi:10.1038/s41374-018-0149-x
43. Mizokami A, Kawakubo-Yasukochi T, Hirata M. Osteocalcin and its endocrine functions. Biochem Pharmacol. 2017;132:1-8. doi:10.1016/j.bcp.2017.02.001
44. Viguet-Carrin S, Garnero P, Delmas PD. The role of collagen in bone strength. Osteoporos Int. 2006;17(3):319-36. doi:10.1007/s00198-005-2035-9
45. Tanaka K, Kanazawa I, Yamaguchi T, Yano S, Kaji H, Sugimoto T. Active vitamin D possesses beneficial effects on the interaction between muscle and bone. Biochem Biophys Res Commun. 2014;450(1):482-7. doi:10.1016/j.bbrc.2014.05.145
46. Bu J, Du J, Shi L, Liu H, Li M. Eldecalcitol effects on osteoblastic differentiation and function in the presence or absence of osteoclastic bone resorption. Exp Ther Med. 2019;18(3):2111-21. doi:10.3892/etm.2019.7784
47. Bemenderfer TB, Harris JS, Condon KW, Li J, Kacena MA. Processing and sectioning undecalcified murine bone specimens. Methods Mol Biol. 2021;2230:231-57.
48. Takahashi N. Mechanism of inhibitory action of eldecalcitol, an active vitamin D analog, on bone resorption in vivo. J Steroid Biochem Mol Biol. 2013;136:171-4. doi:10.1016/j.jsbmb.2012.11.010
49. Kikuta J, Kawamura S, Okiji F, Shirazaki M, Sakai S, Saito H, et al. Sphingosine-1-phosphate-mediated osteoclast precursor monocyte migration is a critical point of control in antibone-resorptive action of active vitamin D. Proc Natl Acad Sci U S A. 2013;110(17):7009-13. doi:10.1073/pnas.1218799110
50. Mi B, Yan C, Xue H, Chen L, Wang X, Wang Y, et al. Inhibition of circulating miR-194-5p reverses osteoporosis through Wnt5a/β-catenin-dependent induction of osteogenic differentiation. Mol Ther Nucleic Acids. 2020;21:814-23. doi:10.1016/j.omtn.2020.07.023
51. Gu Q, Tian H, Zhang K, Chen L, Wang Y, Chen Z, et al. Wnt5a/FZD4 mediates the mechanical stretch-induced osteogenic differentiation of bone mesenchymal stem cells. Cell Physiol Biochem. 2018;48(1):215-26. doi:10.1159/000491721
52. Stakheev D, Taborska P, Strizova Z, Podrazil M, Bartunkova J, Smova K, et al. The WNT/β-catenin signaling inhibitor XAV939 enhances the elimination of LNCaP and PC-3 prostate cancer cells by prostate cancer patient lymphocytes in vitro. Sci Rep. 2019;9(1):4761. doi:10.1038/s41598-019-41182-5
53. Almeida M, Han L, Ambrogini E, Weinstein RS, Manolagas SC. Glucocorticoids and tumor necrosis factor α increase oxidative stress and suppress Wnt protein signaling in osteoblasts. J Biol Chem. 2011;286(52):44326-35. doi:10.1074/jbc.M111.283481
54. Sato AY, Cregor M, Delgado-Calle J, Condon KW, Allen MR, Peacock M, et al. Protection from glucocorticoid-induced osteoporosis by anti-catabolic signaling in the absence of sost/sclerostin. J Bone Miner Res. 2016;31(10):1791-802. doi:10.1002/jbmr.2869
55. Dong Y, Jesse AM, Kohn A, Gunnell LM, O'Keefe RJ, Hilton MJ, et al. RBPjkappa-dependent Notch signaling regulates mesenchymal progenitor cell proliferation and differentiation during skeletal development. Development. 2010;137(9):1461-71. doi:10.1242/dev.042911
56. Brack AS, Conboy IM, Conboy MJ, Shen J, Rando TA. A temporal switch from notch to Wnt signaling in muscle stem cells is necessary for normal adult myogenesis. Cell Stem Cell. 2008;2(1):50-9. doi:10.1016/j.stem.2007.10.006
57. Boulter L, Govaere O, Bird TG, Radulescu S, Ramachandran P, Pellicoro A, et al. Macrophage-derived Wnt opposes Notch signaling to specify hepatic progenitor cell fate in chronic liver disease. Nat Med. 2012;18(4):572-9. doi:10.1038/nm.2667
58. Takebe N, Miele L, Harris PJ, Jeong W, Bando H, Kahn M, et al. Targeting Notch, Hedgehog, and Wnt pathways in cancer stem cells: clinical update. Nat Rev Clin Oncol. 2015;12(8):445-64. doi:10.1038/nrclinonc.2015.61